This is a repository copy of *Impact of phosphate dosing on the microbial ecology of drinking water distribution systems: fieldwork studies in chlorinated networks*.

White Rose Research Online URL for this paper:
http://eprints.whiterose.ac.uk/167039/

Version: Published Version
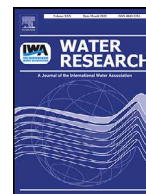
Impact of phosphate dosing on the microbial ecology of drinking water distribution systems: Fieldwork studies in chlorinated networks

I. Douterelo [a,*], B.E. Dutilh [b], C. Calero [a], E. Rosales [a], K. Martin [c], S. Husband [a]

[a] Pennine Water Group, Department of Civil and Structural Engineering, Sir Frederick Mappin Building, University of Sheffield, Sheffield, S1 3JD, United Kingdom
[b] Theoretical Biology and Bioinformatics, Science for Life, Utrecht University, Hugo R. Kruytgebouw, Padualaan 8, 3584, CH, Utrecht, Netherlands
[c] Dwr Cymru Welsh Water, Pentwyn Road, Nelson, Treharris, Mid Glamorgan CF46 6LY, United Kingdom

ABSTRACT

Phosphate is routinely dosed to ensure regulatory compliance for lead in drinking water distribution systems. Little is known about the impact of the phosphate dose on the microbial ecology in these systems and in particular the endemic biofilms. Disturbance of the biofilms and embedded material in distribution can cause regulatory failures for turbidity and metals. To investigate the impact of phosphate on developing biofilms, pipe wall material from four independent pipe sections was mobilised and collected using two twin-flushing operations a year apart in a chlorinated UK network pre- and post-phosphate dosing. Intensive monitoring was undertaken, including turbidity and water physico-chemistry, traditional microbial culture-based indicators, and microbial community structure via sequencing the 16S rRNA gene for bacteria and the ITS2 gene for fungi. Whole metagenome sequencing was used to study shifts in functional characteristics following the addition of phosphate.

As an operational consequence, turbidity responses from the phosphate-enriched water were increased, particularly from cast iron pipes. Differences in the taxonomic composition of both bacteria and fungi were also observed, emphasising a community shift towards microorganisms able to use or metabolise phosphate. Phosphate increased the relative abundance of bacteria such as *Pseudomonas, Paenibacillus, Massilia, Acinetobacter* and the fungi *Cadophora, Rhizophagus* and *Eupenicillium*. Whole metagenome sequencing showed with phosphate a favouring of sequences related to Gram-negative bacterium type cell wall function, virions and thylakoids, but a reduction in the number of sequences associated to vitamin binding, methanogenesis and toxin biosynthesis. With current faecal indicator tests only providing risk detection in bulk water samples, this work improves understanding of how network changes effect microbial ecology and highlights the potential for new approaches to inform future monitoring or control strategies to protect drinking water quality.

1. Introduction

Phosphate is routinely used as a corrosion inhibitor in drinking water distribution systems (DWDS) in order to form highly insoluble phosphate scales that coat pipe walls preventing iron and lead corrosion products entering the water supply (Cardew, 2008). Lead is regarded as a health risk due to the way it can build up in the body, affecting particularly infants and children where it can have an adverse impact on mental development (Lidsky and Schneider, 2003; Verstraeten et al., 2008). A reported 95% of water supplies in the UK phosphate enrich drinking water at concentrations of typically 1 mg P/l (Hayes and Hydes, 2012). There is however a growing shift to try and reduce the use of chemical additives, including phosphate, to drinking supplies but this is currently constrained by historical and regulatory precedence and fears of potential consequences due to limited understanding.

Even though phosphate is not considered harmful to humans, elevated concentrations in aquatic ecosystems can promote microbial and algae growth leading to eutrophication (Glibert, 2020). DWDS are aquatic ecosystems with a diverse microbiota that colonises pipe walls forming biofilms (Flemming et al., 2002). Biofilm growth is affected by different parameters, such as

* Corresponding author.
E-mail address: i.douterelo@sheffield.ac.uk (I. Douterelo).

hydraulic regime, disinfectant residuals temperature and available nutrients including organic carbon, nitrogen and phosphorus (Vrouwenvelder et al., 2010; Liu et al., 2016). Phosphate and chlorine can modify the composition of microbial communities (Batte et al., 2003), thus influencing biofilm formation and the amount of available organic matter and rates of disinfectant decay that ultimately determine the formation of disinfection by products (Chandy et al., 2001). Besides disinfection, the limiting of nutrients, in particular organic carbon, is considered beneficial for controlling microbial growth in drinking water systems (van der Kooij et al., 2003). Volk and LeChevallier, 1999 showed that microbial growth was inhibited in DWDS by reducing the level of organic carbon, but in the short-term the impact was greater on planktonic microorganisms than biofilms. Although carbon is typically the principal limiting nutrient in DWDS, phosphorus can also limit microbial growth (Miettinen et al., 1997; Sathasivan et al., 1997). The impact of phosphate on the drinking water microbiome has been studied using laboratory pipe systems, yielding contradictory results about the effect of phosphate on microorganisms and/or biofilms. Some studies have shown that the addition of phosphates may trigger bacterial growth (Miettinen et al., 1997; Sathasivan et al., 1997; Jang et al., 2012), while other studies did not observe an increase in the growth or number of bacteria (Appenzeller et al., 2001; Frias et al., 2001; Gouider et al., 2009). In some cases, limiting phosphate has been shown to control biofouling of reverse osmosis membranes (Vrouwenvelder et al., 2010). These contradictory results might be associated to different experimental conditions, for example Appenzeller et al. (2001) found a decrease in heterotrophic bacteria growth when phosphate was added in highly corroded iron pipes, but a moderate increase in slightly corroded pipes. However, the research reported was mainly limited to laboratory studies and characterised specific microorganisms using standard culturing methods.

The work presented here avoids these limitations by investigating the microbial impact of phosphate in an operational network using a holistic approach and includes advanced molecular techniques such as whole metagenome sequencing to study functional traits. This information will help to understand the ecological impact of phosphate and to inform network dosing as part of lead or iron control in DWDS. In addition, the results may assist utilities concerned about the potential impact of ceasing phosphate dosing in DWDS, which has associated benefits including reducing treatment complexities (e.g. pH control), chemical purchasing, storage needs and critically as part of protecting the environment against eutrophication risks by removing the need for downstream phosphate removal.

2. Materials and methods

2.1. Study sites and flushing scheme

The studied site is from an operational DWDS in the UK where high lead and iron concentrations were reported as part of routine network sampling. Phosphate dosing was installed to ensure regulatory compliance and prevent future health concerns. Orthophosphoric acid (Phosphoric acid 75% PWG, Airedale Chemical Company Ltd, UK) was dosed in order to achieve a final water concentration of 1.2 mg/l (sampling from 2018 to 2020, $\bar{x} = 1.18$, SD = 0.11 mg/l, $n = 71$). Pre-dosing orthophosphate as P showed all samples from 2017 < 0.03 mg/l ($n = 25$). The new dosing regimen presented an opportunity to examine the impact of phosphate on developing biofilms, including mix-species microbial composition and potential functional traits, in sections of different pipe materials both pre- and post-phosphate dosing. To achieve this a detailed trial plan was proposed that required 4 controlled and extensively monitored flushing operations. Research has shown that

particulate material in DWDS accumulates on all boundary surfaces as part of a biofilm matrix with cohesive shear strength properties (Husband et al., 2016). Accumulation rates are a factor of background water quality, with processes such as corrosion increasing asset deterioration rates with respect to discolouration and associated elevated metal concentrations (Husband et al., 2008). By raising the shear stress (the component of stress coplanar to the pipe surface, a function of hydraulics, pipe diameter and pipe roughness) above daily peak values, material is lifted from the pipe wall and entrained into the bulk flow. This behaviour is commonly observed following network bursts or other interventions that result in modified hydraulic demands but is also utilised in flushing and flow conditioning exercises (Sunny et al., 2020). Due to the shear strength characteristics, the amount of material mobilised is related to the imposed excess shear stress (as a function of the additional flow) and with each subsequent increase there is a further release of material. As a particulate response, the amount of material in the bulk flow can be measured by optical scattering as turbidity. The material release responses have been shown to be predictable and repeatable, including consistent patterns and magnitudes when given equal development periods and stable water quality (Husband et al., 2008; Vreeburg et al., 2008).

With this understanding of network and pipe wall material behaviour, flushing trials were planned with an initial visit to condition test sections by removing material with shear strengths below that of a target flushing flow rate. Biofilm and associated material were then allowed to develop for three months before a second flushing trial was performed to mobilise the regenerated material that was collected for detailed analysis. This twin-flushing process was scheduled to occur prior to phosphate addition (trials 1 and 2) and then repeated once dosing was established (trials 3 and 4). With the aim to investigate the impact of phosphate dosing, environmental factors such as temperature and seasonal/daily demands were minimised by conducting the trials a year apart and using the same equipment and at the same time of the day. The trial flow increases were monitored and controlled by purpose-built Langham hydrant standpipes with electromagnetic ABB Aquamaster 3 flow meters with ±5% reading accuracy and maximum working pressure of 12 bar. Turbidity responses connected to the standpipes were measured using 2x ATI Nephnet loggers for data validity with infrared (IR) Nephelometric measurement and functioning range limited to 0–4.000 NTU for high resolution in one unit and 0–40.00 NTU in the second unit, both with an accuracy of ±5% of reading.

In standard flushing operations, it is normal to maintain a clean waterfront by ensuring all upstream pipe sections are flushed first. This needs to be done otherwise when downstream flushing flows are imposed, the extra demand may exceed upstream conditioned values, causing material to be mobilised and hence consumer water quality issues. Yet any network interventions may also potentially disturb test sections, whilst upstream flushing could also release material that could affect the composition/community on downstream pipes. To avoid this and minimise resource requirements to 1 day, pipe test sections were connected directly to a larger supply pipe to safeguard against the risk that planned flushing trials would cause upstream impact. Through collaboration with the water company, 4 trial sections were identified for field work, with the added advantage that they were of different pipe compositions; medium density polyethylene (MDPE), asbestos cement (AC), polyvinyl chloride (uPVC) and cast iron (CI). Although this study focusses on comparing independent pipe sections pre and post dosing, by selecting trial sections in close proximity and supplied directly from a common trunk main, water entering each pipe section was effectively comparable. The first three sections (MDPE, AC & uPVC) were all supplied directly from the single surface water treatment works via a 21″ AC trunk main.

The fourth section, 2 km further downstream, or one-hour extra transit time, was via an extra 18″ section of spun iron (SI) trunk main (both trunk mains were laid in 1987, so established biofilm and long-term accumulated material could be assumed relatively consistent). With all four trial sections linked directly to effectively the same trunk main (i.e. no intermediary pipe lengths or different pipe materials), it meant the bulk water entering each had the same source, treatment and transmission experience, thereby limiting the impact of bulk water as an experimental variable. The high demands through the trunk main and the close proximity of all test sections meant water age and residual chlorine concentrations were also comparable. Trial sections had diameters in the small range of 75 mm to 125 mm (3″ to 5″) and were 300 m or more in length, except the MDPE pipe. Pipe properties were; MDPE 85 m of 125 mm laid 1995, AC 300 m of 4″ (100 mm) laid 1962, uPVC 420 m of 3″ (75 mm) laid 1967 & CI 300 m of 4″ (100 mm) laid 1953). With the exception of the uPVC which was a dead-end, each pipe supplied downstream networks and experienced daily demand patterns with peak flows of around 10 l/s. Each pipe was over 20 years in service and water company records indicated no flushing or disturbance within the last 10 years, allowing an assumption that pipe wall material and communities were well established and in equilibrium with the system (site schematics and more details in Douterelo et al., 2020).

With trial sections feeding downstream consumers, flushing flows were selected using the PODDS (Prediction of Discolouration in Distribution Systems) model (Husband and Boxall, 2010; Furnass et al., 2014). This identified flows to exceed daily peak, but limit material mobilisation to prevent the particulate turbidity response in the bulk water from producing customer observable discolouration (UK regulatory limit at the customer's tap is 4 NTU, whilst circa 10 NTU is required to start becoming visible). To investigate differences in shear characteristics and to increase discrete sample numbers for analysis and comparison purposes, flushing was planned initially to have three incremental steps with increases occurring once turbidity responses dropped. However, because time constrained to 1-day, on-site decisions based on tracking turbidity responses meant trials 2–4 were reduced to just two steps. Once equipment was installed on-site, a low flow through the standpipe was established and run for a minimum of 20 min to allow monitoring equipment to stabilise and ensure any stagnant water from the hydrant was removed. This was confirmed by ensuring residual chlorine was present.

2.2. Water quality monitoring

The sixteen flushing trials involved an adapted standpipe to control flushing discharge through selected hydrants at the end of each pipe section with visual displays and logging of flow and turbidity. Water samples prior to flush commencement and at each flushing stage were collected for physico-chemical and microbiological analysis. Several parameters were measured *in-situ* at the times of discrete sample collection prior and during flushing of the pipes. Free and total chlorine were measured with a Palintest method using electrochemical sensors and a Palintest CS 100 Chlorosense Chlorine metre (Fisher Scientific, UK). Temperature and pH were measured using a Hanna portable metre and probe HI 991003. All other parameters were obtained by an accredited laboratory analysis of the discrete samples and using validated methods to meet UK drinking water regulations. Water samples were collected in designated containers and bacterial colony counts were determined by the pour-plate method in which yeast extract agar was used following the UK Environment Agency recommendations (Environment Agency, 2012). Cultures were incubated at 37 °C for 48 h (2-day colony) and 22 °C for 72 h (3-day colony).

2.3. Microbial molecular analysis

The molecular microbial approach used in this study is based on two different sequencing strategies. To study the structure (taxonomic composition) of all the samples obtained before and after phosphate dosing ($n = 78$), two marker genes were sequenced; 16S rRNA for bacteria and the ITS2 for fungi. In addition, selected samples based on turbidity results, from each type of material were pooled (total number of final samples = 8, 4 pre- and 4 post-phosphate dosing) and DNA concentrated to perform a whole metagenomics sequencing analysis. Details of each of these analyses are described as follows:

2.3.1. DNA extraction

Three replicates of 2 L samples of bulk water were collected as discrete samples during the flushing trials for DNA analysis from both pre- and post-phosphate dosing (trials 2 and 4). Including collecting background samples before flushing commenced, for the MDPE pipe this meant 4 samples and 3 for the AC, uPVC and CI sections, giving a total of 78 samples. These samples were each filtered through 0.22 μm nitrocellulose membrane filters (Millipore, Corp). Filters were preserved in the dark and at −80 °C for subsequent DNA extraction. DNA extraction from filters was carried out by a method based on proteinase K digestion followed by a standard phenol/chloroform-isoamyl alcohol extraction (Douterelo et al., 2013). The quantity and purity of the extracted DNA were assessed using Nanodrop ND-1000 spectrophotometer (NanoDrop, Wilmington, USA).

2.3.2. Sequencing of marker genes (16S rRNA for bacteria and ITS2 for fungi)

Sequencing was performed at MR DNA (www.mrdnalab.com, Shallowater, TX, USA) on a MiSeq following the manufacturer's guidelines. The 16S rRNA gene using primers 28F and 519R spanning the V1 to V3 hypervariable regions and primers targeting the ITS1–2 regions were used for bacterial and fungal analysis, respectively. The PCR conditions and Illumina library preparation are explained in detail in Douterelo et al., 2020. Sequencing data was processed using MR DNA analysis pipeline (MR DNA, Shallowater, TX, USA). In summary, sequences were joined and depleted of barcodes then sequences with less than 150 bp and with ambiguous base calls were removed. Sequences were de-noised, and chimeras were detected using UCHIME (Edgar et al., 2011) and removed from further analysis. Final Operational Taxonomic Units (OTUs) were taxonomically classified using BLASTn (Altschul et al., 1990) against a curated database derived from RDPII (Cole et al., 2005) and NCBI. To study alpha-diversity (diversity within samples) the Chao rich estimator, Shannon diversity analysis and Dominance estimators were calculated at 95% sequence similarity cut off (Douterelo et al., 2013), without rarefaction (McMurdie and Holmes, 2014).

2.3.3. Whole metagenome sequencing

To obtain a fingerprint of functional traits, selected samples based on peaks of turbidity during flushes, were pooled and subjected to whole metagenome sequencing. 50 ng of DNA was used to prepare the libraries by Nextera DNA Sample preparation (Illumina) following the manufacturer's user guide and the sequencing was performed at MR DNA (www.mrdnalab.com, Shallowater, TX, USA) on MiSeq following the manufacturer's guidelines as described by Douterelo., 2020.

Eight libraries (MDPE, AC, uPVC, and CI, all sampled before and after phosphate treatment) were quality checked with FastQC (https://www.bioinformatics.babraham.ac.uk/projects/fastqc/) and cross-assembled with metaSPAdes v.3.11.0 (Nurk et al., 2017). Comparative metagenomic analysis based on this cross-assembly was performed with crAss (Dutilh et al., 2012). Con-

tig abundance was calculated by mapping the reads back to the contigs using BWA-MEM (Li and Durbin, 2009), and calculating the average depth with the jgi_summarize_bam_contig_depths script from MetaBAT (Kang et al., 2015). Contigs were annotated with InterProScan 5.36–75.0 with the parameters: –appl Pfam –goterms –iprlookup –pathways (https://github.com/ebi-pf-team/interproscan, (Jones et al., 2014) and summarized using the metagenomics ontology of GO Slim (http://geneontology.org/docs/download-ontology/). Abundance of the functional categories was calculated for each sample by summing the depth values of the contigs where it occurred and the values log-10 transformed (pseudocount: 0.0001, see Supplementary Table 1). Because the crAss cladograms indicated separation of the samples into groups before/after phosphate treatment (Fig. 5), overall enrichment scores per functional category due to the phosphate treatment were calculated by averaging the values across the four pipe materials.

2.4. Statistics

To assess the similarity in microbial community structure amongst samples, the relative sequence abundance at genus level (97% sequence similarity cut-off) for each sample was used to calculate pairwise similarities. All data were transformed by square root calculations and Bray–Curtis similarity matrixes were generated using the software Primer v7 (PRIMER-E, Plymouth, UK). Bray–Curtis similarity matrixes were visualised using multiple-dimensional scaling (MDS) diagrams. Analysis of similarity statistics (ANOSIM) was calculated using the same Bray–Curtis distance matrix to test the significance of differences amongst samples based on pipe material for both bacteria and fungi. The values for the ANOSIM R-statistic ranges from -1 to 1, where $R = 1$ indicates that communities from different pipe materials are completely dissimilar. Principal component analysis (PCA) was used to evaluate the distribution of microorganisms taking into account materials and phosphate dosing generated using the software Primer v7 (PRIMER-E, Plymouth, UK).

To determine if the observed differences in the richness, diversity and dominance indeces were significant, pairwise comparisons between samples from different materials were made using the non-parametric Mann–Whitney U test using IBM SPSS 21.

3. Results

3.1. Flushing flow and turbidity

Each investigative visit (4 over two years) and flushing operations (4 per visit, approximately 1 hour each including incremental increases) were completed in one day with initial pre-dosing conditioning trial (1) in March 2017 followed after 90 days biofilm/material development by the sample collection/analysis trial (2). Phosphate dosing at the treatment works commenced 5 months later (November 2017). Following a field-operative call-out on the scheduled date, the post-dosing conditioning trial (3) was delayed a month until April 2018 with the sample collection trial (4) after biofilm development again exactly 90 days later. Prior to and during the investigative period no significant network events were recorded or changes in network demands or operation other than phosphate dosing coming on-line. Sampling results, including free chlorine, water temperature and DOC from the water treatment works, highlight network supplied water quality, and therefore likely particulate material loading, to be consistent across both generation phases, as shown in Fig. 1. Although water temperature at the start is the same for both years, during 2018 it does however rise quicker (a cold spell just before the final flushing visit brings temperatures back in-line). Flow and turbidity results from all four flushing trials for each pipe section are shown in Fig. 2

(plots show times adjusted to create a common start time with a maximum 63-minute shift required to align all 16 trials). In all cases imposed hydraulics were comparable for all flushes, except the MDPE pipe where flush 2 & 4 had higher flows (Fig. 2A). With trials 1 and 3 however the same, applied hydraulics are consistent for both phases of the trial and therefore results remain comparable. In the AC pipe (Fig. 2B), during trial 4 the terminal step was 4 L/s compared to 3.4 L/s from trial 2. Trials in both the uPVC and CI pipes (Figs. 2C and 2D respectively) had consistent flow magnitudes but some variance in durations, in particular the terminal flushing phase as a result of waiting for turbidity values to drop to agreed levels of 0.5 NTU before finishing. These temporal differences however would be not expected to impact turbidity responses. More details on the hydraulic properties and results from the first two trials can be found in Douterelo et al., 2020.

Initial inspection of the turbidity responses observed from all pipe sections suggests that the addition of phosphate considerably increases discolouration risk. The mean turbidity results for each pipe and trial are reported in Table 1. In every pipe a greater turbidity response is observed once phosphate dosing has commenced, supporting the initial observation that phosphate enrichment increases discolouration risk. Comparison between materials of the pipe sections showed similar turbidity increases for MDPE and AC pipes, where both sections were hydraulically similar (2.1x and 1.5x respectively). The CI pipe showed by far the greatest increase in turbidity (4.7x), suggesting changes in corrosion or corrosion legacy, thus suggesting metallic corrosion remains an issue despite the presence of phosphate. The dead-end pipe, where material accumulation can be considered predominantly a sedimentation process and not biofilm formation on walls, showed almost no change (1.1x), suggesting that the bulk water material loading (background concentrations) is largely unaffected.

3.2. Discrete sampling and physico-chemical analysis

Results from the physico-chemical analysis of discrete water samples are showed in Table 2. Given the common water source supply, many physico-chemical variables were similar amongst all the samples including pH (7.6–7.8), conductivity (240–250 μS/cm), nitrite (<0.004 mg/L) and sulphate (8.6–9.5 mg/L). However, changes were found in some physico-chemical parameters between the first sample period in June 2017 and the second period a year later after phosphate dosing. The quantification of orthophosphate confirms that water in the first sampling period had no/little phosphate (<0.03 mg/L), whilst one year later this had increased to 1.1–1.2 mg/L, which is the average UK standard water phosphate concentration. TOC and DOC were higher and more variable, going from 1.9–2.0 mg/L to 2.4–2.7 mg/L and 2.0–2.1 mg/L to 2.4–3.2 mg/L respectively post-phosphate addition. Nitrate were 0.52–0.54 mg/L in the first sampling period and decreased until not being detected (<0.5) after phosphate dosing. Chlorine (both free and total) was higher under post-phosphate dosing conditions in most of the samples analysed with the exception of MDPE samples where it was slightly higher pre-phosphate (0.7–1.1 mg/l). Temperature, in the second sampling period was slightly higher and increased across the trial periods from an average of 18 °C to 21.30 °C.

In pre-phosphate dosing water, iron concentrations were significantly higher in the CI pipe and the uPVC pipe samples when compared with other pipe materials. Post-phosphate dosing higher iron concentrations were found in MDPE and AC pipes when compared with pre-phosphate conditions. In addition, iron increased in the last flushing step in the AC pipe after phosphate dosing. Manganese concentration was stable in most of the conditions (0.012–0.053 mg/L), and it was slightly higher in the final flushing steps in both CI and AC pipes in post-phosphate samples. Lead concentra-
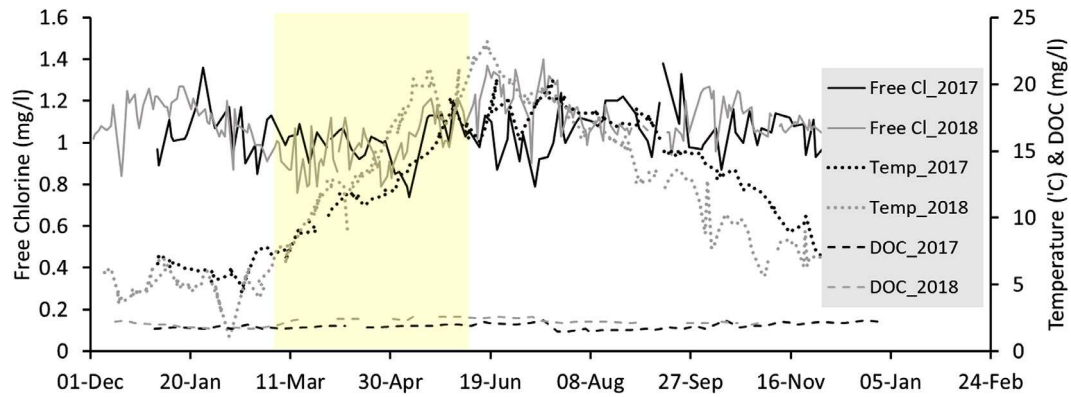
Fig. 1. Treated water quality parameters (free chlorine, temperature and DOC) supplying the test sections during 2017 and 2018. Trial period is highlighted. Note 2018 values have been shifted back 25 days to allow direct comparison during the 90 day biofilm and material accumulation period.
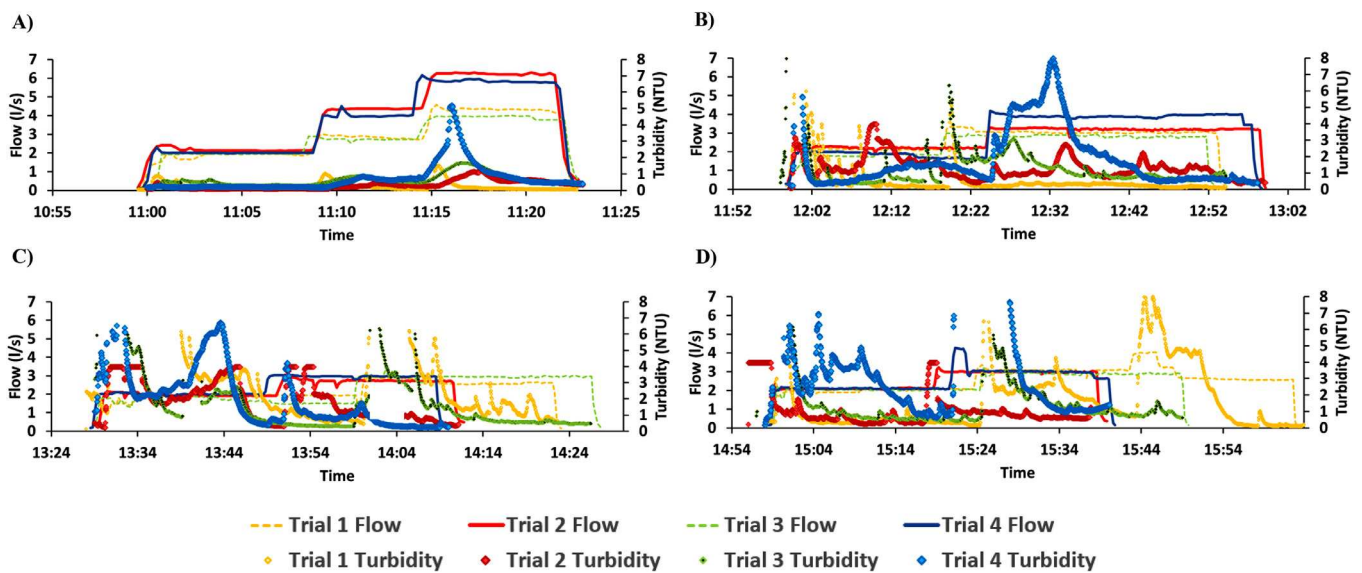
Fig. 2. Flow and Turbidity results from 4 x flushing trials for each test section with A = MDPE, B = AC, C= uPVC & D = CI.

Table 1
Mean turbidity for each pipe section per trial.

Pipe	Mean Turbidity (NTU)/pipe section/trial			
	Trial 1	Trial 2	Trial 3	Trial 4
MDPE	0.23	0.33	0.62	0.70
AC	0.50	1.28	2.26	1.90
uPVC	7.62	1.90	3.67	2.12
CI	2.12	1.05	4.19	4.96
Trial 1 & 2, separated by 90 days are pre-phosphate dosing. Trial 3 & 4, also 90 days apart, have phosphate dosed supply				

Table 2

Physico-chemical analysis of water from different materials under pre (-P) or post (+ P) phosphate addition conditions.

Material	pH -P	pH +P	Conductivity 20 °C (µS/cm) -P	+P	Turbidity (NTU) -P	+P	Mn (mg/l) -P	+P	Fe(mg/l) -P	+P	TOC (mg/l) -P	+P	Nitrate (mg/l) -P	+P	Nitrite (mg/l) -P	+P	Ortophosphate as P (mg/l) -P	+P	Sulphate (mg/l) -P	+P	DOC (mg/l) -P	+P	Lead (mg/l) -P	+P	Chlorine (Free) (mg/l) -P	+P	Chlorine (total) (mg/l) -P	+P
MDPE	7,7	7,7	240	250	0,11	0,08	0,01	0,0059	0,01	0,016	1,90	2,7	0,54	<0,5	<0,004	<0,004	<0,03	1,2	9,1	9	2,1	2,7	0,00018	0,00008	0,76	0,99	0,76	1,22
MDPE	7,7	7,6	240	240	0,06	0,42	0,01	0,028	0,01	0,065	1,90	2,4	0,54	<0,5	<0,004	<0,004	<0,03	1,2	9,2	9	2	2,4	0,00009	0,0001	0,76	1,01	0,98	1,04
MDPE	7,7	7,7	240	240	0,18	0,31	0,02	0,023	*	0,047	2,00	2,4	0,55	<0,5	<0,004	<0,004	<0,03	1,2	9,2	9	2,1	2,5	0,00013	0,00012	0,72	1,1	0,74	1,3
MDPE	7,7	7,7	240	240	0,66	0,1	0,04	0,0049	0,10	0,031	1,90	2,7	0,52	<0,5	<0,004	<0,004	<0,03	1,2	9,1	9,1	2,1	2,4	0,00019	0,00018	1,01	1,1	1,10	1,3
AC	7,8	7,7	240	240	0,06	0,15	0,01	0,013	0,02	0,067	1,90	2,4	0,55	<0,5	<0,004	<0,004	<0,03	1,2	9,5	9	2	3,2	0,00007	0,00022	0,40	1,1	0,60	1,3
AC	7,8	7,7	240	250	0,37	2,8	0,01	0,1	0,09	0,78	1,90	2,4	0,52	<0,5	<0,004	<0,004	<0,03	1,2	9	8,9	2	2,4	0,00030	0,00057	0,60	1,08	1,10	1,2
AC	7,7	7,7	240	240	0,54	0,73	0,02	0,025	0,12	0,19	1,90	2,4	0,53	<0,5	<0,004	<0,004	<0,03	1,1	9,3	8,9	2	2,4	0,00011	0,00011	0,85	0,87	1,00	0,92
uPVC	7,7	7,7	240	240	0,20	2,4	0,01	0,043	*	0,44	1,90	2,6	0,54	<0,5	<0,004	<0,004	<0,03	1,1	9,1	8,8	2	2,4	0,00005	0,00054	0,73	0,97	0,90	1,2
uPVC	7,7	7,7	240	240	4,40	0,48	0,05	0,013	0,97	0,33	1,90	2,4	0,52	<0,5	<0,004	<0,004	<0,03	1,2	9,1	8,4	2	2,4	0,00140	0,00028	0,80	1,09	0,80	1,3
uPVC	7,7	7,7	240	240	1,80	0,14	0,03	0,0048	0,61	0,028	1,90	2,4	0,53	<0,5	<0,004	<0,004	<0,03	1,1	9,1	8,7	2	2,9	0,00066	0,00022	0,87	0,87	0,88	1,1
CI	7,7	7,8	240	240	3,00	2,2	0,01	0,047	0,39	0,39	1,90	2,7	0,53	<0,5	<0,004	<0,004	<0,03	1,2	9,2	8,9	2,1	2,7	0,00005	0,00014	0,68	1,05	0,92	1,1
CI	7,7	7,8	240	240	0,29	7	0,02	0,49	0,05	0,9	1,90	2,5	0,52	<0,5	<0,004	<0,004	<0,03	1,2	9,8	8,5	2	2,4	0,00005	0,0007	0,93	1,03	0,92	1,2
CI	7,7	7,6	240	240	0,70	0,8	0,02	0,053	0,17	0,098	1,90	2,5	0,53	<0,5	<0,004	<0,004	<0,03	1,2	8,6	9	2	2,7	0,00005	0,00015	0,75	1,09	1,00	1,1

*No data obtained

Table 3

Results from microbial-culture dependant colonies count pre- (-P) and post-phosphate (+P) for each type of material pipe.

Material_Flushing Step	Colonies 7 days 22 °C (c/ml) -P	+P	Colonies 3 days 22 °C (c/ml) -P	+P	Colonies 2 days 37 °C (c/ml) -P	+P
MDPE_1	2	1	0	0	0	0
MDPE_2	0	1	0	0	0	0
MDPE_3	0	0	0	0	0	0
MDPE_4	0	13	2	3	0	1
AC-1	7	21	4	1	0	0
AC-2	1	5	0	1	1	0
AC-3	0	1	0	0	0	0
uPVC_1	0	0	0	0	0	0
uPVC_2	0	2	1	0	0	0
uPVC_3	0	0	0	1	0	0
CI-1	3	42	0	0	0	0
CI-2	0	0	0	0	1	0
CI-3	0	1	0	0	0	0

tion was similar amongst all the samples except in the last flushing steps after phosphate dosing were increased in AC and CI pipes and decrease in the uPVC pipe.

Results from the colony counts are shown in Table 3. Colony counts values were only representative in samples from the AC pipe, with up to 7 colonies per mL at 22 °C for 7 days and 4 colonies at 22 °C for 3 in pre-phosphate samples. However, up to 21 colonies per mL at 22 °C for 7 days and up to 3 colonies at 22 °C for 3 days were found under phosphate concentrations. Also, 42 colonies per mL at 22 °C for 7 days were count in the CI pipe and 13 in the final flushing stage of MDPE pipe in post-phosphate addition samples.

3.2. Effect of phosphate on microbial community composition (before vs. after): taxonomic analysis based on marker genes 16S rRNA and ITS2 for bacteria and fungi respectively

Differences in the taxonomic composition of both bacteria and fungi were found in relation to phosphate dosing, pipe material and flushing steps.

3.2.1. Bacterial relative abundance at genus level

The relative abundance of the most abundant OTUs at genus level (95% similarity cut off) has been analysed comparing the flushing steps in different materials and pre- and post-phosphate dosing (Figs. 3 and 4). Independently of pipe material or phosphate concentration, the first flushing step generally resulted in samples with higher relative abundance of bacterial and fungal communities. The proceeding flushing steps were less microbial rich (bacteria and fungi). Concerning phosphate dosing, bacterial communities showed a higher relative abundance in pre-phosphate dose samples, whilst the opposite was observed for fungi. The results observed from Figs. 3 and 4 were reinforced by the diversity indices data (Fig. 7).

The bacterial analysis (Fig. 3) showed that the most represented genera in all the samples was *Pseudomonas* with a relative abundance between 4 and 21% in pre-phosphate samples and ranging from 4 to 32% under post-phosphate dosing. An increase in abundance of *Pseudomonas* post-phosphate was observed particularly in AC and CI pipe samples. Other genera well represented in pre-phosphate samples were *Gloeobacter* (2–14%) and *Staphylococcus* (3–14%). However, in post-phosphate samples, *Gloeobacter* almost disappeared (0–2%) and *Staphylococcus* was mainly present in MDPE pipe samples (4–17%) but noticeably diminished in AC, uPVC and CI pipe samples. *Acinetobacter* was relatively abundant in MDPE samples, particularly in the last flushing steps under pre-phosphate dosing (>10%, suggesting preference to deeper and more consolidated biofilm colonisation niche). This genus had lit-
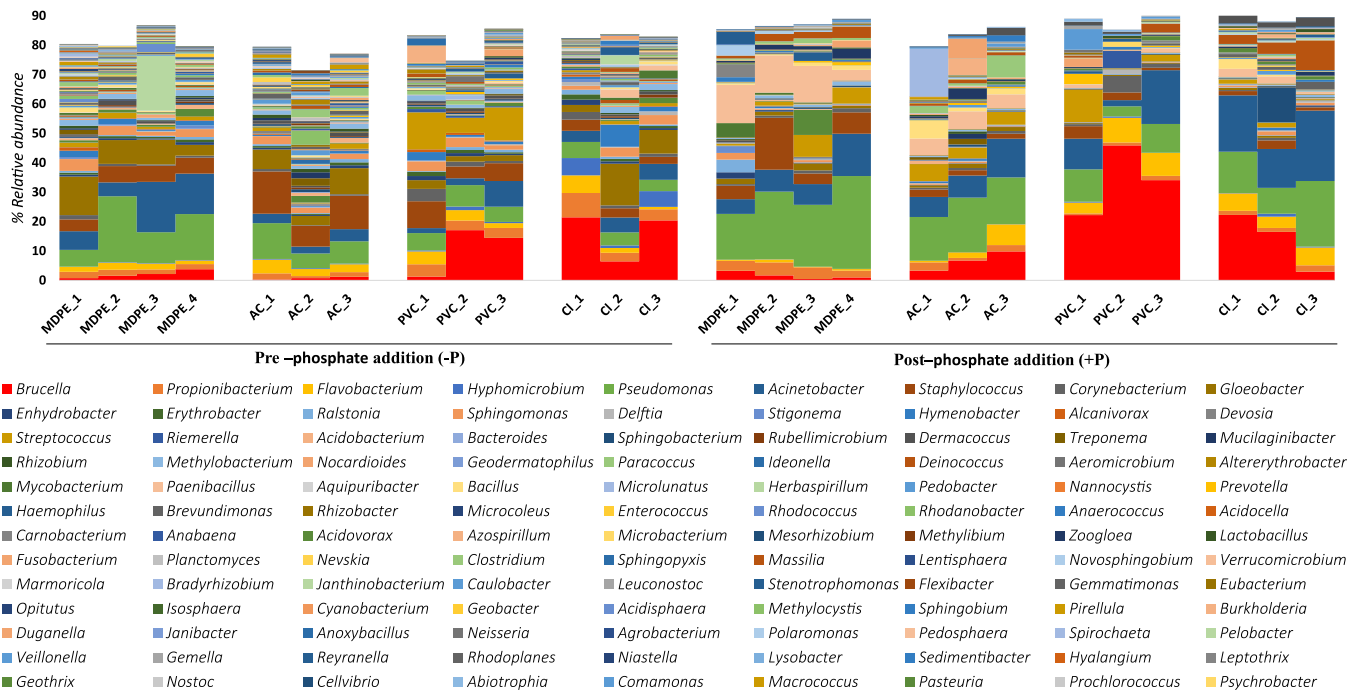
Fig. 3. Percentage of relative abundance of bacteria at genus level for each of the flushing steps (average of 3 replicates, $n = 3$), materials and under pre-phosphate (<0.03 mg/l) or post-phosphate conditions (1.1–1.2 mg/l). Numbers on the pipe materials labels indicate the flushing step.
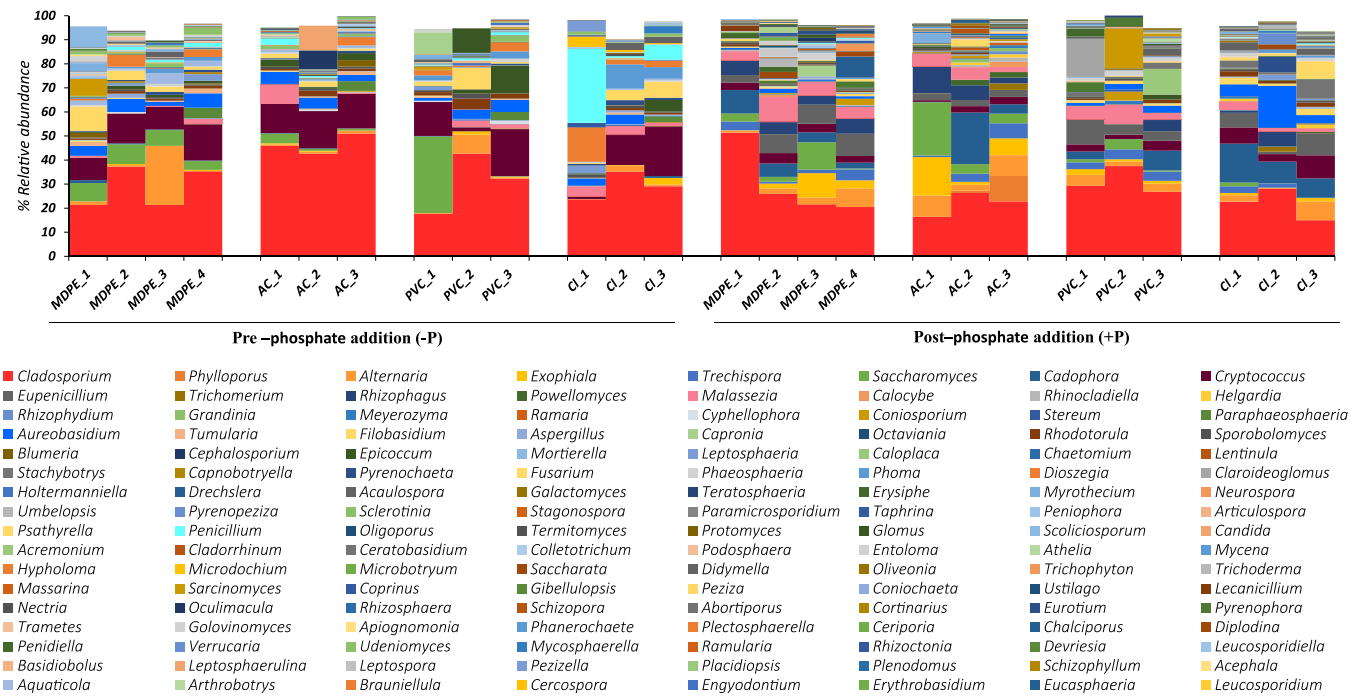

Fig. 4. Percentage of relative abundance of fungi at genus level for each of the flushing steps (average of 3 replicates, $n = 3$), materials and under pre-phosphate (<0.03 mg/l) or post-phosphate conditions (1.1–1.2 mg/l). Numbers on the pipe materials labels indicate the flushing step.

tle representation in AC, PVC and CI pipe pre-phosphate, but increased abundance in post-phosphate samples, especially in CI (13–24%). Other genus that had little representation (0–2%) in all pre-phosphate samples but increased post-phosphate was *Paenibacillus*. *Paenibacillus* (post-phosphate), showed high relative abundance in MDPE samples in the first flushing steps (12–13%) and in the first flushing step of other materials (2–5%), but was then poorly represented (suggesting a colonisation preference for outer

layers of developing DWDS biofilms when phosphate is prevalent). B*rucella*, in pre-phosphate uPVC samples, ranged from 1% in the first flushing step to 14% in the last one. In CI samples, *Brucella* was also relatively abundant (7–21%) in pre-phosphate samples and decreased to 3% in the last flushing step post-phosphate. In pre-phosphate samples and uPVC, *Streptococcus* have higher abundance (5 to 12%) when compared with samples from other materials. After phosphate addition, *Streptococcus* was still present in AC
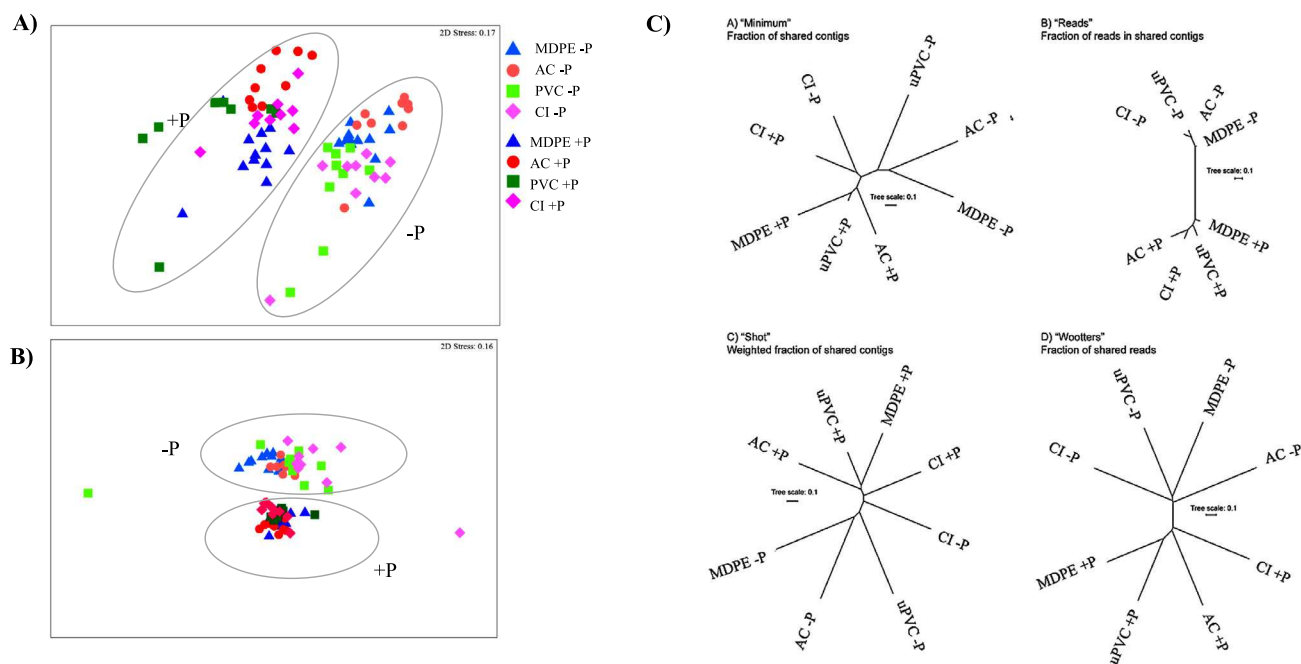
Fig. 5. Two-dimensional plot of the multidimensional scaling (MDS) analysis based on Bray–Curtis similarities of the percentage abundance **(A)** bacteria and **(B)** fungi. Showing differences in the bacterial community structure between pre-phosphate (<0.03 mg/l) or post-phosphate dose conditions (1.1–1.2 mg/l). (n = 39). Symbols are representing individual samples and are coloured based on sample type. **C)** Cladograms representing the distance between metagenomes based on A) the fraction of shared contigs, B) fractions of reads in shared contigs, C) the weighted fraction of shared contigs and D) shared fractions of shared reads between all sample pairs performed with crAss.

(6–4%), CI (2–0%) and uPVC samples (0–11%) and MDPE samples (0.6% in the first flushing step to 7% in the last one).

3.2.2. Fungal relative abundance at genus level

The analysis of fungal communities (Fig. 4), showed that in pre-phosphate samples *Cladosporium* (from 15 to 51%) was present in all the samples. Remarkably, pre-phosphate AC samples showed relative abundances of 43% to 51%. *Cryptococcus* was the second most abundant genus in pre-phosphate samples (average 12%, n = 13), yet its presence decreased after phosphate dosing (1–6%), and only showing a relative abundance of 10% in the last flushing step in CI samples. Under pre-phosphate dosing conditions, other abundant genera were *Saccharomyces*, in MDPE samples (average 7%, n = 4), and in the first flushing steps of AC and uPVC (4% and 32%, respectively); *Aureobasidium,* had a relative abundance of 3–4% in MDPE, AC and CI samples; *Penicillium* in CI (30% in the first flush); and *Alternaria* in MDPE (25% in the third flushing stage).

Under post-phosphate conditions, *Saccharomyces* was also represented in MDPE (average 4%, n = 4), and in AC (changing from 22% to 4% as the flushing steps moved forward); *Cadophora* was represented in all samples ranging from 1 to 22%, being more abundant in AC and CI; and *Exophiala* in MDPE (average 4%, n = 4) and AC (average 8%, n = 3) samples. *Rhizophagus* was a genus with no representation under pre-phosphate conditions but it was found ranging from 1 to 11% in all water samples post- phosphate.

3.2.3. Non-metric multidimensional scaling (MDS) analysis of bacteria and fungi and cross-assembly analysis of whole metagenome sequencing with crAss

MDS plots of the relative abundance of bacteria at 95% sequence similarity cut off, showed a clear separation between pre- and post-phosphate dosing and all different pipe materials, even though some outliers were found (Fig. 5A). The analysis of similarities (ANOSIM) confirmed the differences amongst bacterial community structures (Global R = 0.654, p = 0.1%).

Differences also were found in fungal structure between phosphate conditions (Global R = 0.56, p = 0.1%), but only between some pipe materials (Fig. 5B). Pre-phosphate, fungal community structure was significantly different between MDPE and AC pipes (R = 0.258, p = 0.3%); MDPE and PVC pipes (R = 0.317, p = 0.1%); MDPE and CI pipes (R = 0.389, p = 0.1%); and AC and CI pipes (R = 0.275, p = 0.3%). Post-phosphate showed significant differences only between MDPE and CI pipes (R = 0.336, p = 0.2%); and AC and CI pipes (R = 0.408, p = 0.1%).

The differences amongst microbial community structures were further supported by comparative metagenomics analysis (i.e. similarities between metagenomes). The cross-assembly analysis with crAss using whole metagenomics reads was represented using cladograms (Fig. 5C), These show many cross-contigs that exclusively contain reads from pre- or post-phosphate metagenomes, independently of the pipe material analysed. Notably, the pre- and post-treatment phosphate samples were sequenced in separate batches, so potential batch effects could not be ruled out (Leek et al., 2010).

3.2.4. Principal component analysis (PCA)

PCA analysis was performed in bacterial and fungal communities using data from relative abundance at 95% sequence similarity cut off (Fig. 6). PCA indicated that generally samples clustered together as function of phosphate dosing. In both bacteria and fungi, a clear separation between pre- and post-phosphate addition samples were observed and some genera had affinity for one or the other condition. Several bacterial genera (Fig. 6A) including *Pseudomonas, Paenibacillus, Massilia, Acinetobacter* had a vector with tendency to appear after phosphate dosing (+P). This trend was also observed for the fungi (Fig. 6B), *Rhizophagus, Eupenicillium, Cadophora and Trechispora.* For bacteria, samples also clustered with respect to pipe material, yet this effect of pipe material was not clear for fungi after phosphate addition.
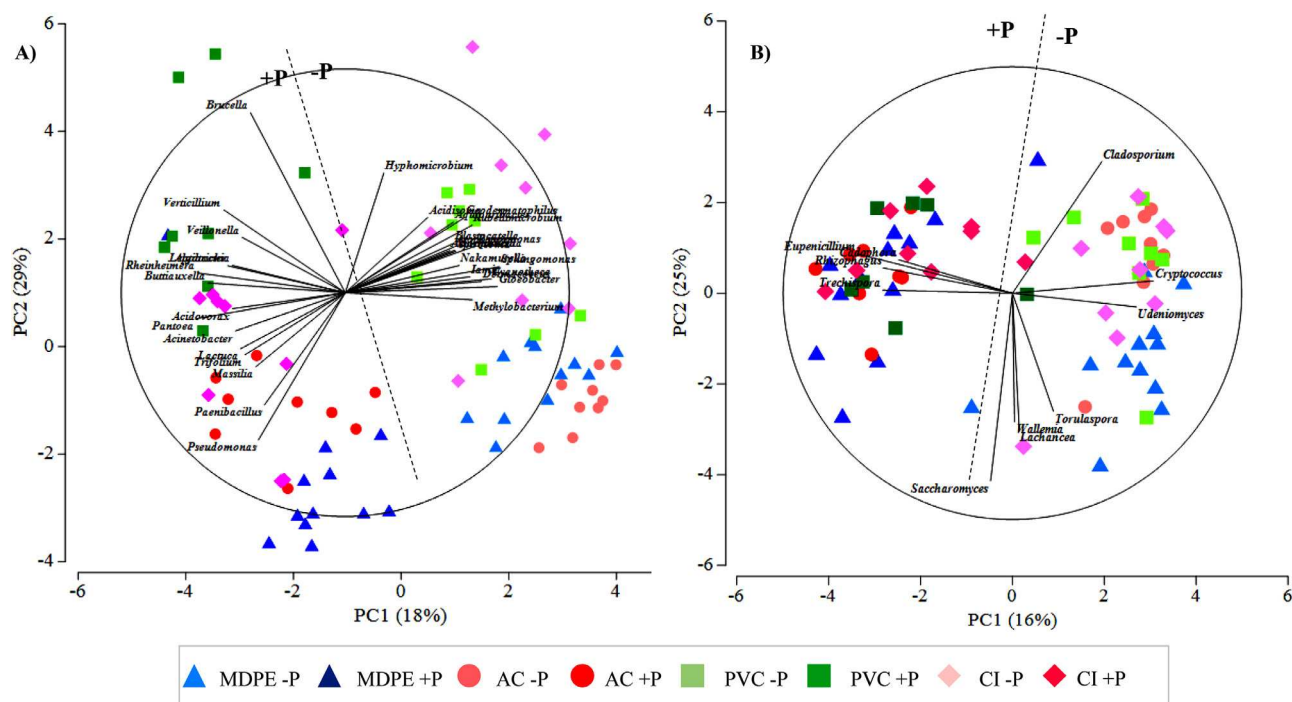
Fig. 6. Principal component analysis (PCA) plot of the percentage abundance (A) bacteria and (B) fungi grown in different materials and pre-phosphate (<0.03 mg/l) or post-phosphate dose conditions (1.1–1.2 mg/l) ($n = 39$). Symbols are representing individual samples and are coloured based on sample type. Percentages on principal components axis represent the amount of variation explained by each PC.

The results indicate that differences in microbial community arise following the addition of phosphate and this occurs irrespective of pipe material.

3.2.5. Bacterial and fungal alpha diversity

Shannon diversity index, dominance and Chao1 richness estimator at genus level for bacteria and fungi were performed (Fig. 7). Overall, bacterial communities were more diverse and rich than fungal communities. Regarding bacteria, significant differences were found in all indices (Shannon, Chao1 and Dominance) between pre- and post- phosphate conditions ($p < 0.05$, $n = 39$). Higher diversity and richness were obtained for bacteria under pre-phosphate conditions, compared to post-phosphate samples. AC samples presented more diversity (average= 3.76, $n = 18$) and lower values for the dominance indicator (average= 0.07, $n = 18$). Lower values were found in pre-phosphate samples for the dominance indicator in bacteria. Regarding this index, significant differences were found between AC and CI in pre-phosphate samples for bacteria ($p < 0.05$) and between MDPE and AC fungi pre-phosphate samples ($p < 0.05$). Fungal communities pre-phosphate dosing were less rich and had higher values for the dominance index than fungi post-phosphate conditions but no differences were found regarding diversity.

3.3. Effect of phosphate on microbial traits and functions

Results for the analysis of whole metagenomics sequencing are showed in Fig. 8. Overall, pre-phosphate samples independently of the pipe material or flush step had higher relative abundance of functional traits associated to biosynthetic process, nucleotidyl transferase activity, and nucleic acid binding and transport activity. When the results of the relative abundance of the functional traits were log transformed (Supplementary Material Table 1); some functional traits that were not present or not well represented in pre-phosphate samples were distinguished for all types of pipe material including: gram-negative bacterium type

cell wall, virion, thylakoid and extrachromosomal circular DNA. However, other functional traits decreased in all samples including quorum sensing, methanogenesis, beta-galactosidase complex, vitamin binding.

4. Discussion

4.1. Effect of phosphate dosing on turbidity and material accumulation on pipe materials

Independently of pipe material or phosphate regime, results showed the first flushing step generally resulted in samples with higher microbial relative abundance. This result could be expected as biofilm mobilised in the first flushing step can be considered as the outer layer that is exposed to the highest exchange with the bulk flow, including nutrient and planktonic cell transfer (Donlan, 2002). While the underlying biofilm layers with more consolidated conditions and lower transfer potential, are less diverse and more resistant to detachment (Paul et al., 2012; Douterelo et al., 2013). It is generally considered that diverse microbial communities are better at resisting and adapting to environmental changes due to functional redundancy (Allison and Martiny, 2008). The outer layers therefore provide a barrier helping to maintain conditions and protect against mobilisation of material consolidated in underlying zones. In addition, the metabolically active outer biofilm layers may prevent the immediate effectiveness of phosphate dosing by breaking up and slowing the formation of resilient and protective insoluble lead phosphates scales. With the rapid increase of hydraulic forces during flushing, deeper biofilm layers become exposed to new conditions. As these communities adapt or break down, material previously trapped can be released, resulting in higher turbidity as observed (Table 1). The generally higher turbidity after flushing post-phosphate dosing could also be attributable to the newly developing biofilm having an enhanced capability of cellular growth and/or extracellular polymeric substance (EPS) production. This would enable greater
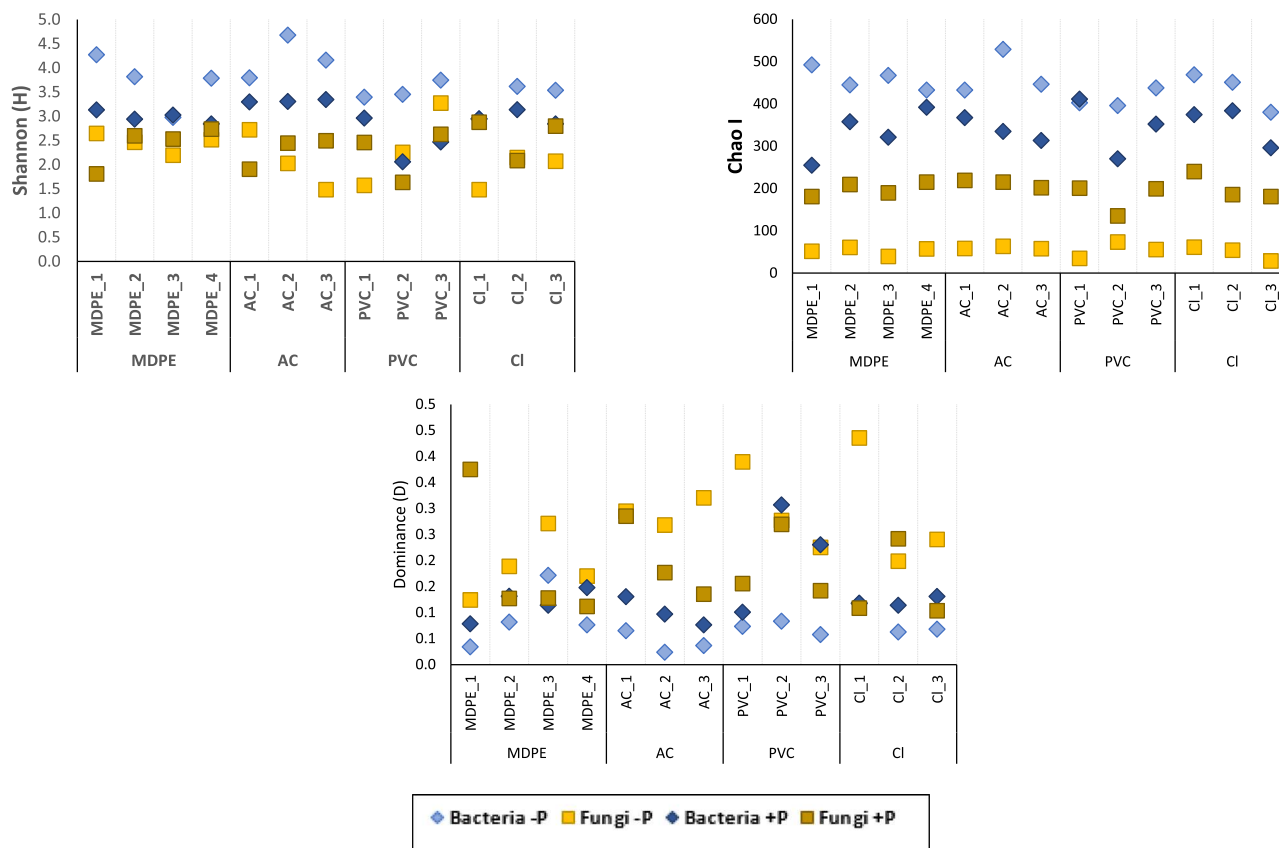
Fig. 7. Diversity index (Shannon), Chao I (richness index) and Dominance for OTUs at 95% cut off for bacteria (blue markers) and fungi (orange markers) under pre-phosphate (<0.03 mg/l; -P) or post-phosphate conditions (1.1–1.2 mg/l; +P). Names on axis Y are pipe material (MDPE, AC, PVC and CI), numbers are flushing step (1 to 4) (n = 3).

material trapping and retention (Flemming et al., 2016). However, without cells or EPS quantification, this observation on more rapid biofilm growth and/or increased EPS production yielding enhanced material capture cannot be confirmed. EPS contains compounds that participate in biofilm adhesion and several studies in drinking water agree that when phosphate content increases, the production of EPS decreases (Fang et al., 2010; Kirisits et al., 2013; Noh et al., 2019). If EPS production is reduced by phosphate addition, it could be argued biofilm capability to adhere to pipes will be reduced, allowing easier removal and hence a reason for the higher turbidities observed. The effect of phosphate on EPS production could explain the increased turbidity response from the CI pipe post-phosphate, preventing the rapid action of phosphate forming protective scales and allowing high concentrations of corrosion by-products.

Historically, phosphate addition is recognised as beneficial to reduce plumbosolvency of drinking water, hence the higher turbidity response observed in this study could be linked to a transitional period that will recover once phosphate adapted microbial communities have been established. Further trials would be key to test this and are recommended, especially with initial findings showing the addition of phosphate has not reduced iron or lead concentrations as expected. A key recommendation to water utilities would be to ensure that where changes in the network are planned, preceding maintenance or cleaning strategies are undertaken to minimise biofilm impact. This would remove accumulated pipe wall material capable of causing both short- and long-term risk, and in the case of preventative chemical remediation (such as phosphate dosing to build protective scales) allow more rapid penetration and greater effectiveness.

4.2. Phosphate dosing effect on microbial community structure

Considering the influence of phosphate on material mobilised from pipe walls, clear differences were found between pre- and post- phosphate dosing samples, particularly for bacterial communities. Bacteria were the main drivers of changes in biofilm community structure, in terms of richness and diversity. Bacterial communities showed a higher relative abundance in pre-phosphate dose samples, whilst the opposite was observed for fungi. Previous studies have observed that bacterial communities were more affected by environmental fluctuations than fungi within biofilms in chlorinated DWDS (Douterelo et al., 2018). This study supports this trend and shows higher environmental influence on bacteria occurring in biofilms attached to a range of materials used in DWDS.

The analysis of bacterial relative abundance showed clear taxonomic differences related to phosphate dosing in all type of materials. Higher diversity and richness were obtained pre-phosphate for bacteria when compared with post-phosphate conditions. This study shows how phosphate acts as a selective force for microorganisms, favouring those able to use or metabolise phosphate. Many microorganisms are able to transform phosphate in polyphosphates (PolyP) and accumulate it in their cells (Boswell et al., 2001). In fact, there is a phenomenon called "luxury uptake of phosphorous/phosphate" in which bacteria accumulate PolyP under phosphate excess conditions, even though it might not be favourable for their growth (Khoshmanesh et al., 2002; Hirota et al., 2010). In this study, higher abundance of *Acinetobacter* members were found in post-phosphate samples and it has been reported that *Acinetobacter* are important in phosphorus removal strategies in wastewater treatment plants (Kim et al.,

Fig. 8. Functional analysis based on whole metagenomics sequencing of samples before and after phosphate dosing.

1997; Bunce et al., 2018). Similarly, *Paenibacillus* present in this study has been related to solubilisation of phosphate in soils (Arthurson et al., 2011). The PCA analysis (Fig. 6) showed that some genera, such as *Pseudomonas, Paenibacillus, Massilia*, and *Acinetobacter* were clearly influenced by phosphate and these genera have been linked to solubilisation or accumulation of phosphate in previous studies (van Groenestijn et al., 1988; Boswell et al., 2001, Zheng et al., 2017). Fungi such as *Rhizophagus* increased their abundance after phosphate dosing, and this fungi is known to establish symbiotic interactions with plants to help phosphate uptake (Fiorilli et al., 2013). *Rhizophagus* and *Eupenicillium* were clearly influenced by phosphate addition in this study, and they have been previously related to phosphate solubilisation in a range of environments (Vyas et al., 2007; Garcia et al., 2017). Previous studies indicated that certain materials used to build drinking water infrastructure can leach out polymers that fungi can degrade (Belila et al., 2017), a possible explanation for the high relative abundance of some organisms in this study. For example, *Penicillium* and *Fusarium* are known biodegraders of natural and synthetic polyethylene (Ojha et al., 2017), and have great potential for removal of pharmaceutical compounds (Olicón-Hernández et al., 2017). Since biofilm formation on pipes is unavoidable, further research is now needed to determine if the occurrence of specific inter-kingdom interactions can promote beneficial biofilms and aid biodegradation of contaminants in these systems.

The most common group of microorganisms in all the samples, but with different relative abundance depending on the pipe material and flushing step, were *Pseudomonas, Acinetobacter* and *Sphingomonas* and in CI pipes *Brucella*. Niquette et al. (2000), examined the influence of pipe materials on densities of fixed bacterial

biomass in DWDS, showing that biomass on plastic (PVC and PE) were lowest in comparison with iron, and that cement-based materials had intermediate values. Conversely, other researchers have shown that plastic, including PE, can stimulate biofilm growth due to the release of biodegradable compounds that can promote microbial growth (Van der Kooij et al., 2005; Yu et al., 2010). The results from this study indicate that pipe material affects microbial communities, in particular bacteria, and those differences were mainly between corroding and non-corroding materials.

4.3. Effect of phosphate dosing on functional traits and metagenomes

Most of the sequences analysed were related to biofilm development and resistant mechanisms. Overall three main functional traits were characterised; biosynthetic process, nucleic acid binding and nucleotide transferase activity (Fig. 8). Biosynthetic process in biofilms are mainly related with EPS production and related to functions such as cell attachment, formation and maintenance of biofilm structure and resistance to environmental stress, including disinfectants (Hall-Stoodley and Stoodley, 2002). Regarding nucleic acid binding, these sequences are associated to proteins that bind to DNA/RNA and include transcriptional factors, which modulate protein expression (Hudson and Ortlund, 2014). Nucleotidyltransferases are enzymes within the transferases group, which are associated to an extensive class of bacterial enzymes that inhibit antibiotic target binding, promoting its inactivation (Wright, 2005; Schroeder et al., 2017).

The analysis of interrelationships between metagenomes showed clear differences between pre- and post-phosphate treatments (Fig. 5C). Mapping metagenomic sequences to a refer-

ence database is a useful approach to transfer taxonomical and functional annotations to sequence reads. However, it can limit the amount of data that can be analysed since most sequencing reads in difficult-to-annotate datasets (e.g. viral metagenomes) lack known homologs (Dutilh et al., 2012). An alternative is using reference-independent comparative metagenomics by cross-assembly through crAss. The cross-assembly analysis showed that the effect of the phosphate addition was stronger than the effect of the pipe material, since the before and after samples clustered together. Phosphate dosing favoured the presence of sequences related to functional traits, in particular Gram-negative bacterium type cell walls, virions, thylakoids and extrachromosal circular DNA (Supplementary Table 1). Gram-negative bacteria are predominant inhabitants of drinking water systems and include Proteobacteria members and the phylum Bacteroidetes (Vaz-Moreira et al., 2017). Gram-negative bacteria have an outer membrane that makes them resistant to antibiotics, detergents and disinfectants (McKeon et al., 1995), thus are of public health concern. Very high rate of resistance to antibiotics have been found amongst Gram-negative bacteria and within them Enterobacteriaceae since they have a more fluid genome, mediated by plasmids that carry antibiotic resistance and pathogenicity genes (Wellington et al., 2013; Hawkey, 2015). This reinforces our results where higher abundance of sequences associated with extrachromosomal circular DNA were observed after phosphate dosing. Extrachromosomal circular DNA are a type of Mobile Genetic Elements (MGE) that facilitate DNA transfer between cells and can provide host cells with advantages, such as antibiotic resistance or adaptive metabolic pathways (Rankin et al., 2011). It is known that mixed-species biofilms in DWDS can house antibiotic resistance bacteria (Gomez-Alvarez et al., 2016; Douterelo et al., 2018), thus biofilm mobilisation may contribute to spreading environmental antimicrobial resistance. Additionally, Gram-negative bacteria are known to have enhanced adhesion capabilities (Sommer et al., 1999), promoting biofilm spread and colonisation. Taking into account these findings, phosphate addition is shown to have potentially detrimental consequences, that may be of concern to public health, on the distribution system microbiome.

Virions were more represented in all samples post-phosphate dosing. They are commonly transported in drinking water systems by amoebas (Atanasova et al., 2018), where they are protected against the action of disinfectants. Flood and Ashbolt (2000), have demonstrated the potential of model enteric virions and virion-sized particles to accumulate and persist within biofilms in drinking water systems. This study only analysed DNA, thus it is not known if the sequences associated to virions are a realistic representation of these type of microorganisms in biofilms. The results obtained however support the need for more detailed microbial analysis in routine drinking water monitoring strategies, with surveillance methods needing to take into consideration the accumulation of virions and other potential pathogens within water pipe biofilms.

Sequences associated with thylakoids were also prevalent post-phosphate dosing (Fig. 8). Thylakoids are organelles which contains pigments that absorb energy in photosynthetic organisms and have been used as a fast and effective screening test to detect herbicides in water (Euzet et al., 2005). The presence of thylakoids can also indicate the increase of photosynthetic microorganisms such as cyanobacteria in biofilms of DWDS. Cyanobacteria have been found in this study; however no significant increase was observed in post-phosphate dosing samples. Cyanobacteria have been reported previously as important inhabitants of biofilms in DWDS (Hwang et al., 2012; Lin et al., 2013; Douterelo et al., 2016), and despite the lack of light it has been suggested that they have an alternative metabolism that allows them to survive in the absence of light.

Sequences associated with functional traits that decreased in all samples after phosphate dosing include quorum sensing, methanogenesis, beta-galactosidase complexes and vitamin binding (Fig. 8). Quorum sensing is a mechanism common in biofilms, where cells regulate their cooperative activities and physiological processes by releasing, sensing and responding to small diffusible signal molecules (Li and Tian, 2012). Therefore, phosphate dosing might influence the ability of bacteria to communicate and subsequently form biofilms, and as discussed above phosphate can inhibit EPS production. If phosphate addition is involved or has an indirect role in quorum sensing mechanisms and their control, this may open a new avenue for controlling biofilm formation in DWDS. Beta-galactosidase complexes are hydrolytic enzymes responsible for the degradation of a variety of natural and synthetic substrates (Asraf and Gunasekaran, 2010), thus biofilms may use them to degrade a range of compounds and thrive in DWDS. Phosphate dosing also decreased methanogenesis, which is the final step in anaerobic degradation of carbon and is used by microorganisms to degrade carbon when all alternative electron acceptors have been exhausted (Zeikus, 1977). Methanogens are amongst the most diverse groups of microbes and vary significantly in their environmental conditions and cell structure. In the literature, methanogens are well known bio-degraders of micropollutants, and most belong to the group of Archaea (Harb et al., 2019). Archaea have been found in drinking water systems, mainly in systems supplied from groundwater and associated to ammonia-oxidation (Van der Wielen et al., 2009). Although phosphate dosing decreased sequences associated to methanogenesis, this study cannot directly associate this with a reduction in the number of Archaea.

Phosphate addition decreased functional sequences related to vitamin binding. Vitamins and other cofactors play a critical role in determining bacterial growth rates and microbiome dynamics (Sonnenburg and Sonnenburg, 2014). The importance of vitamin acquisition and the mechanisms that microbes use to acquire these vitamins have been reported in other environments (Putnam et al., 2020). Vitamins can play a critical role in driving microbiome dynamics, and competition for vitamins can favour bacteria that are better at capturing those. Studies based on single species biofilms showed vitamin-related processes can influence biofilm formation and development. Pandit et al. (2017), studying *Pseudomonas aeruginosa* biofilms, suggested that non-lethal concentrations of vitamin C can inhibit bacterial quorum sensing and other regulatory mechanisms involved in biofilm development. As a result, EPS biosynthesis is reduced and once content is below a critical point, cells get exposed and are more susceptible to antimicrobials or treatments. Considering these previous studies, a reduction of vitamin binding function in a DWDS context could be translated as selection for certain type of microorganisms (supporting reduced diversity observed post- phosphate) and/or influence EPS structure and microbiome susceptibility to environmental conditions. Further studies are needed to understand how vitamin acquisition shapes competition and community structure under DWDS environmental conditions and appreciate vitamin binding implications at an operational and management level.

5. Conclusions

This innovative research investigates the effect of phosphate dosing on the microbial ecology within an operational DWDS. The detailed study plan facilitated investigation of the impact of pipe material and hydraulics on developing biofilms. Following changes in water chemistry due to phosphate enrichment, the work highlights differences in microbial diversity and functional traits and demonstrates clear operational impact with respect to discolouration risk. Key findings include:

- Differences in the taxonomic composition of both bacteria and fungi were found in relation to phosphate dosing, pipe material and flushing steps;
  - Bacterial communities showed a higher relative abundance diversity and richness in pre-phosphate dose samples, whilst the opposite was observed for fungi
  - Cast iron pipe samples had less diverse communities with dominant representatives compared to other non-corroding pipes
  - First flushing steps resulted in samples with higher relative abundance of bacterial and fungal communities
- Post-phosphate dosing a community shift towards microorganisms able to use or metabolise phosphate was observed, including the bacteria *Pseudomonas, Paenibacillus, Massilia, Acinetobacter* and the fungi *Cadophora, Rhizophagus* and *Eupenicillium.*
- Addition of phosphate favoured the appearance of Gram-negative bacterium type cell wall, virion and thylakoid function sequences, but decreased functional sequences associated to vitamin binding, methanogenesis and toxin biosynthesis.
- Operationally, turbidity responses (discolouration and elevated metal concentration risk) from the phosphate enriched water was increased, particularly from cast iron pipes.

With current faecal indicator tests only providing risk detection, this work improves understanding and highlights the potential for new approaches based on genetic data to inform future monitoring or control strategies to protect drinking water quality.

Declaration of Competing Interest

None.

Acknowledgment

Supplementary materials

Supplementary material associated with this article can be found, in the online version, at doi:10.1016/j.watres.2020.116416.

References

Allison, S.D., Martiny, J.B.H., 2008. Resistance, resilience, and redundancy in microbial communities. Proceed. National Academy Sciences 105, 11512.

Altschul, S.F., Gish, W., Miller, W., Myers, E.W., Lipman, D.J., 1990. Basic local alignment search tool. J. Mol. Biol. 215, 403–410.

Appenzeller, B., Batté, M., Mathieu, L., Block, J., Lahoussine, V., Cavard, J., Gatel, D., 2001. Effect of adding phosphate to drinking water on bacterial growth in slightly and highly corroded pipes. Water Res 35, 1100–1105.

Arthurson, V., Hjort, K., Muleta, D., Jäderlund, L., Granhall, U., 2011. Effects on Glomus mosseae root colonization by Paenibacillus polymyxa and Paenibacillus brasilensis strains as related to soil P-availability in winter wheat. Applied and Environmental Soil Science 2011.

Asraf, S.S., Gunasekaran, P., 2010. Current trends of ß-galactosidase research and application. In: Current research, Technology and Education Topics in Applied Microbiology and Microbial Biotechnology. Microbiology book series Formatex Research Center, Spain, pp. 880–890.

Atanasova, N.D., Dey, R., Scott, C., Li, Q., Pang, X.-.L., Ashbolt, N.J., 2018. Persistence of infectious Enterovirus within free-living amoebae – A novel waterborne risk pathway. Water Res 144, 204–214.

Batté, M., Mathieu, L., Laurent, P., Prévost, M, 2003. Influence of phosphate and disinfection on the composition of biofilms produced from drinking water, as measured by fluorescence in situ hybridization. Can J Microbiol 49 (12), 741–753. doi:10.1139/w03-094, 2003.

Belila, A., El-Chakhtoura, J., Saikaly, P.E., van Loosdrecht, M.C.M., Vrouwenvelder, J.S., 2017. Eukaryotic community diversity and spatial variation during drinking water production (by seawater desalination) and distribution in a full-scale network. Environmental Science: Water Research Techno. 3, 92–105.

Boswell, C., Dick, R., Eccles, H., Macaskie, L., 2001. Phosphate uptake and release by Acinetobacter johnsonii in continuous culture and coupling of phosphate release to heavy metal accumulation. J. industrial microbiology and biotechnology 26, 333–340.

Bunce, J.T., Ndam, E., Ofiteru, I.D., Moore, A., Graham, D.W., 2018. A Review of Phosphorus Removal Technologies and Their Applicability to Small-Scale Domestic Wastewater Treatment Systems. Frontiers in Environmental Science 6.

Cardew, P.T., 2008. Measuring the benefit of orthophosphate treatment on lead in drinking water. J Water Health 7, 123–131.

Chandy, J.P., Angles, M.L., 2001. Determination of nutrients limiting biofilm formation and the subsequent impact on disinfectant decay. Water Res. 35 (11), 2677–2682.

Cole, J.R., Chai, B., Farris, R.J., Wang, Q., Kulam, S.A., McGarrell, D.M., Garrity, G.M., Tiedje, J.M., 2005. The Ribosomal Database Project (RDP-II): sequences and tools for high-throughput rRNA analysis. Nucleic Acids Res. 33, D294–D296.

Donlan, R.M., 2002. Biofilms: microbial life on surfaces. Emerg Infect Dis 8, 881–890.

Douterelo, I., Sharpe, R.L., Boxall, J.B., 2013. Influence of hydraulic regimes on bacterial community structure and composition in an experimental drinking water distribution system. Water Res 47, 503–516.

Douterelo, I., Fish, K.E., Boxall, J.B., 2018a. Succession of bacterial and fungal communities within biofilms of a chlorinated drinking water distribution system. Water Res 141, 74–85.

Douterelo, I., Husband, S., Loza, V., Boxall, J., 2016. Dynamics of Biofilm Regrowth in Drinking Water Distribution Systems. Appl Environ Microb 82, 4155–4168.

Douterelo, I., Dutilh, B.E., Arkhipova, K., Calero, C., Husband, S., 2020. Microbial diversity, ecological networks and functional traits associated to materials used in drinking water distribution systems. Water Res 173, 115586.

Dutilh, B.E., Schmieder, R., Nulton, J., Felts, B., Salamon, P., Edwards, R.A., Mokili, J.L., 2012. Reference-independent comparative metagenomics using cross-assembly: crAss. Bioinformatics 28, 3225–3231.

Edgar, R.C., Haas, B.J., Clemente, J.C., Quince, C., Knight, R., 2011. UCHIME improves sensitivity and speed of chimera detection. Bioinformatics 27, 2194–2200.

Euzet, P., Giardi, M.T., Rouillon, R., 2005. A crosslinked matrix of thylakoids coupled to the fluorescence transducer in order to detect herbicides. Anal. Chim. Acta 539, 263–269.

Fang, W., Hu, J., Ong, S.L., 2010. Effects of phosphorus on biofilm disinfections in model drinking water distribution systems. J Water Health 8, 446–454.

Fiorilli, V., Lanfranco, L., Bonfante, P., 2013. The expression of GintPT, the phosphate transporter of Rhizophagus irregularis, depends on the symbiotic status and phosphate availability. Planta 237, 1267–1277.

Flemming, H.-.C., Percival, S.L., Walker, J.T., 2002. Contamination potential of biofilms in water distribution systems. Water Supply 2, 271–280.

Flemming, H.-.C., Wingender, J., Szewzyk, U., Steinberg, P., Rice, S.A., Kjelleberg, S., 2016. Biofilms: an emergent form of bacterial life. Nature Reviews Microbiology 14, 563–575.

Flood, J., 2000. Virus-sized particles can be entrapped and concentrated one hundred fold within wetland biofilms. Advances in Environmental Research 3, 403–411.

Frias, J., Ribas, F., Lucena, F., 2001. Effects of different nutrients on bacterial growth in a pilot distribution system. Antonie Van Leeuwenhoek 80, 129–138.

Furnass, W., Collins, R., Husband, P., Sharpe, R., Mounce, S., Boxall, J., 2014. Modelling both the continual erosion and regeneration of discolouration material in drinking water distribution systems. Water Science and Technology: Water Supply 14, 81–90.

Garcia, K., Chasman, D., Roy, S., Ané, J.-.M., 2017. Physiological Responses and Gene Co-Expression Network of Mycorrhizal Roots under K+Deprivation. Plant Physiol. 173, 1811–1823.

Glibert, P.M., 2020. Harmful algae at the complex nexus of eutrophication and climate change. Harmful Algae 91, 101583.

Gomez-Alvarez, V., Pfaller, S., Pressman, J.G., Wahman, D.G., Revetta, R.P., 2016. Resilience of microbial communities in a simulated drinking water distribution system subjected to disturbances: role of conditionally rare taxa and potential implications for antibiotic-resistant bacteria. Environmental Science: Water Research Techno. 2, 645–657.

Gouider, M., Bouzid, J., Sayadi, S., Montiel, A., 2009. Impact of orthophosphate addition on biofilm development in drinking water distribution systems. J. Hazard. Mater. 167, 1198–1202.

Hall-Stoodley, L., Stoodley, P., 2002. Developmental regulation of microbial biofilms. Curr. Opin. Biotechnol. 13, 228–233.

Harb, M., Lou, E., Smith, A.L., Stadler, L.B., 2019. Perspectives on the fate of micropollutants in mainstream anaerobic wastewater treatment. Curr. Opin. Biotechnol. 57, 94–100.

Hawkey, P., 2015. Multidrug-resistant Gram-negative bacteria: a product of globalization. J. Hospital Infection 89, 241–247.

Hayes, C.R., Hydes, O.D., 2012. UK experience in the monitoring and control of lead in drinking water. J Water Health 10, 337–348.

Hirota, R., Kuroda, A., Kato, J., Ohtake, H., 2010. Bacterial phosphate metabolism and its application to phosphorus recovery and industrial bioprocesses. J. Biosci. Bioeng. 109, 423–432.

Hudson, W.H., Ortlund, E.A., 2014. The structure, function and evolution of proteins that bind DNA and RNA. Nat Rev Mol Cell Biol 15, 749–760.

Husband, P.S., Boxall, J.B., Saul, A.J., 2008. Laboratory studies investigating the processes leading to discolouration in water distribution networks. Water Res 42, 4309–4318.

Husband, S., Boxall, J.B., 2010. Field Studies of Discoloration in Water Distribution Systems: model Verification and Practical Implications. J. Environmental Engineering 136, 86–94.

Husband, S., Fish, K.E., Douterelo, I., Boxall, J., 2016. Linking discolouration modelling and biofilm behaviour within drinking water distribution systems. Water Sci Tech-W Sup 16, 942–950.

Hwang, C., Ling, F., Andersen, G.L., LeChevallier, M.W., Liu, W.-.T., 2012. Microbial Community Dynamics of an Urban Drinking Water Distribution System Subjected to Phases of Chloramination and Chlorination Treatments. Appl Environ Microb 78, 7856.

Jang, H.J., Choi, Y.J., Ro, H.M., Ka, J.O., 2012. Effects of phosphate addition on biofilm bacterial communities and water quality in annular reactors equipped with stainless steel and ductile cast iron pipes. J. Microbiol. 50, 17–28.

Jones, P., Binns, D., Chang, H.Y., et al., 2014. InterProScan 5: genome-scale protein function classification. Bioinformatics 30, 1236–1240.

Kang, D.D., Froula, J., Egan, R., Wang, Z., 2015. MetaBAT, an efficient tool for accurately reconstructing single genomes from complex microbial communities. PeerJ 3, e1165.

Khoshmanesh, A., Hart, B.T., Duncan, A., Beckett, R., 2002. Luxury uptake of phosphorus by sediment bacteria. Water Res 36, 774–778.

Kim, M.H., Hao, O.J., Wang, N.S., 1997. Acinetobacter isolates from different activated sludge processes: characteristics and neural network identification. FEMS Microbiol. Ecol. 23, 217–227.

Kirisits M.J., Evans A. & Lauderdale C. (2013) Effect of phosphorus limitation on the production of extracellular polymeric substances (EPS) by drinking-water bacteria. p.^pp. 59–63.

Leek, J.T., Scharpf, R.B., Bravo, H.C., Simcha, D., Langmead, B., Johnson, W.E., Geman, D., Baggerly, K., Irizarry, R.A., 2010. Tackling the widespread and critical impact of batch effects in high-throughput data. Nat Rev Genet 11, 733–739.

Li, H., Durbin, R., 2009. Fast and accurate short read alignment with Burrows-Wheeler transform. Bioinformatics 25, 1754–1760.

Li, Y.-.H., Tian, X., 2012. Quorum sensing and bacterial social interactions in biofilms. Sensors 12, 2519–2538.

Lidsky, T.I., Schneider, J.S., 2003. Lead neurotoxicity in children: basic mechanisms and clinical correlates. Brain 126, 5–19.

Lin, W., Yu, Z., Chen, X., Liu, R., Zhang, H., 2013. Molecular characterization of natural biofilms from household taps with different materials: PVC, stainless steel, and cast iron in drinking water distribution system. Appl Microbiol Biot 97, 8393–8401.

Liu, S., Gunawan, C., Barraud, N., Rice, S.A., Harry, E.J., Amal, R., 2016. Understanding, Monitoring, and Controlling Biofilm Growth in Drinking Water Distribution Systems. Environ. Sci. Technol. 50, 8954–8976.

McKeon, D.M., Calabrese, J.P., Bissonnette, G.K., 1995. Antibiotic resistant gram-negative bacteria in rural groundwater supplies. Water Res 29, 1902–1908.

McMurdie, P.J., Holmes, S., 2014. Waste Not, Want Not: why Rarefying Microbiome Data Is Inadmissible. PLoS Comput. Biol. 10, e1003531.

Miettinen, I.T., Vartiainen, T., Martikainen, P.J., 1997. Phosphorus and bacterial growth in drinking water. Appl Environ Microbiol 63, 3242–3245.

Niquette, P., Servais, P., Savoir, R., 2000. Impacts of pipe materials on densities of fixed bacterial biomass in a drinking water distribution system. Water Res. 34, 1952–1956.

Noh, J.H., Yoo, S.H., Son, H., Fish, K.E., Douterelo, I., Maeng, S.K., 2019. Effects of phosphate and hydrogen peroxide on the performance of a biological activated carbon filter for enhanced biofiltration. J. Hazard. Mater., 121778.

Nurk, S., Meleshko, D., Korobeynikov, A., Pevzner, P.A., 2017. metaSPAdes: a new versatile metagenomic assembler. Genome Res. 27, 824–834.

Ojha, N., Pradhan, N., Singh, S., Barla, A., Shrivastava, A., Khatua, P., Rai, V., Bose, S., 2017. Evaluation of HDPE and LDPE degradation by fungus, implemented by statistical optimization. Sci Rep 7 39515–39515.

Olicón-Hernández, D.R., González-López, J., Aranda, E., 2017. Overview on the biochemical potential of filamentous fungi to degrade pharmaceutical compounds. Front. Microbiol. 8, 1792.

Pandit, S., et al., 2017. "Low Concentrations of Vitamin C Reduce the Synthesis of Extracellular Polymers and Destabilize Bacterial Biofilms. Front Microbiol 8.

Paul, E., Ochoa, J.C., Pechaud, Y., Liu, Y., Line, A., 2012. Effect of shear stress and growth conditions on detachment and physical properties of biofilms. Water Res 46, 5499–5508.

Putnam, E.E., Goodman, A.L., 2020. B vitamin acquisition by gut commensal bacteria. PLoS Pathog 16 (1), e1008208. https://doi.org/10.1371/journal.ppat.1008208.

Rankin, D.J., Eduardo, P.C.R., Brown, S.P., 2011. What traits are carried on mobile genetic elements, and why? Heredity 106 (1), 1–10.

Sathasivan, A., Ohgaki, S., Yamamoto, K., Kamiko, N., 1997. Role of inorganic phosphorus in controlling regrowth in water distribution system. Water Science and Technology 35, 37.

Schroeder, M., Brooks, B.D., Brooks, A.E., 2017. The Complex Relationship between Virulence and Antibiotic Resistance. Genes (Basel) 8, 39.

Sommer, P., Martin-Rouas, C., Mettler, E., 1999. Influence of the adherent population level on biofilm population, structure and resistance to chlorination. Food Microbiol. 16 (5), 503–515.

Sonnenburg, E.D., Sonnenburg, J.L, 2014. Gut microbes take their vitamins. Cell Host Microbe 15, 5–6. doi:10.1016/j.chom.2013.12.011, Sommer P, Martin-Rouas C & Mettler E (1999) Influence of the adherent population level on biofilm population, structure and resistance to chlorination. Food Microbiology 16: 503-515.

Sunny, I., Husband, P.S., Boxall, J.B., 2020. Impact of hydraulic interventions on chronic and acute material loading and discolouration risk in drinking water distribution systems. Water Res 169, 115224.

van der Kooij, D., Vrouwenvelder, J.S., Veenendaal, H.R., 2003. Elucidation and control of biofilm formation processes in water treatment and distribution using the Unified Biofilm Approach. Water science and technology: a journal of the International Association on Water Pollution Research 47, 83–90.

Van der Kooij, D., Veenendaal, H.R., Scheffer, W.J., 2005. Biofilm formation and multiplication of Legionella in a model warm water system with pipes of copper, stainless steel and cross-linked polyethylene. Water Res 39, 2789–2798.

Van der Wielen, P.W., Voost, S., van der Kooij, D., 2009. Ammonia-oxidizing bacteria and archaea in groundwater treatment and drinking water distribution systems. Appl Environ Microbiol 75, 4687–4695.

van Groenestijn, J.W., Vlekke, G.J., Anink, D.M., Deinema, M.H., Zehnder, A.J., 1988. Role of cations in accumulation and release of phosphate by Acinetobacter strain 210A. Appl Environ Microbiol 54, 2894–2901.

Vaz-Moreira, I., Nunes, O.C., Manaia, C.M., 2017. Ubiquitous and persistent Proteobacteria and other Gram-negative bacteria in drinking water. Sci Total Environ 586, 1141–1149.

Verstraeten, S.V., Aimo, L., Oteiza, P.I., 2008. Aluminium and lead: molecular mechanisms of brain toxicity. Arch. Toxicol. 82, 789–802.

Volk, C.J., LeChevallier, M.W., 1999. Impacts of the reduction of nutrient levels on bacterial water quality in distribution systems. Appl. Environ. Microbiol. 65 (11), 4957–4966.

Vreeburg, J.H.G., Schippers, D., Verberk, J.Q.J.C., van Dijk, J.C., 2008. Impact of particles on sediment accumulation in a drinking water distribution system. Water Res 42, 4233–4242.

Vrouwenvelder, J.S., Beyer, F., Dahmani, K., Hasan, N., Galjaard, G., Kruithof, J.C., Van Loosdrecht, M.C., 2010. Phosphate limitation to control biofouling. Water Res 44, 3454–3466.

Vyas, P., Rahi, P., Chauhan, A., Gulati, A., 2007. Phosphate solubilization potential and stress tolerance of Eupenicillium parvum from tea soil. Mycol Res 111, 931–938.

Wellington, E.M., Boxall, A.B., Cross, P., Feil, E.J., Gaze, W.H., Hawkey, P.M., Johnson-Rollings, A.S., Jones, D.L., Lee, N.M., Otten, W., 2013. The role of the natural environment in the emergence of antibiotic resistance in Gram-negative bacteria. The Lancet infectious diseases 13, 155–165.

Wright, G.D., 2005. Bacterial resistance to antibiotics: enzymatic degradation and modification. Adv. Drug Deliv. Rev. 57, 1451–1470.

Yu, J., Kim, D., Lee, T., 2010. Microbial diversity in biofilms on water distribution pipes of different materials. Water Science and Technology 61, 163–171.

Zeikus, J., 1977. The biology of methanogenic bacteria. Bacteriol Rev 41, 514.

Zheng, B.-.X., Bi, Q.-.F., Hao, X.-.L., Zhou, G.-.W., Yang, X.-.R., 2017. Massilia phosphatilytica sp. nov., a phosphate solubilizing bacteria isolated from a long-term fertilized soil. Int. J. Syst. Evol. Microbiol. 67, 2514–2519.